Vaccine 38 (2020) 3671–3681

Contents lists available at ScienceDirect

Vaccine

journal homepage: www.elsevier.com/locate/vaccine

Development of a multivalent enterovirus subunit vaccine based on immunoinformatic design principles for the prevention of HFMD

Huixiong Deng [a,b], Shun Yu [a,b], Yingzhu Guo [a,b], Liming Gu [a,b], Gefei Wang [a,b,*], Zhihui Ren [a,c], Yanlei Li [a,b], Kangsheng Li [a,b], Rui Li [a,b,*]

[a] Center of Pathogen Biology and Immunology, Department of Microbiology and Immunology, Shantou University Medical College, Shantou 505041, Guangdong, China
[b] Guangdong Provincial Key Laboratory of Infectious Disease and Molecular Immunopathology, Shantou University Medical College, Shantou 505041, Guangdong, China
[c] Department of Anesthesiology, The Second Xiangya Hospital of Central South University, Changsha 410011, China

ARTICLE INFO

Article history:
Received 21 October 2019
Received in revised form 6 March 2020
Accepted 7 March 2020
Available online 2 April 2020

Keywords:
HFMD
Enterovirus
Multivalent
Epitopes
In silico
Neutralization

ABSTRACT

Hand, foot and mouth disease (HFMD) is mainly caused by EV-A71 and CV-A16. An increasing number of cases have been found to be caused by CV-A10, CV-A6, CV-B3 and the outbreaks are becoming increasingly more complex, often accompanied by the prevalence of a variety of enteroviruses. Based on the principle of synthetic peptide vaccines, we applied immune-informatics to design a highly efficient and safe multivalent epitope-based vaccine against EV-A71, CV-A16, CV-A10, CV-A6 and CV-B3. By screening B-cells, HTL and CTL cell antigen epitopes with high conservativity and immunogenicity that have no toxic effect on the host, further analysis confirmed that the vaccine built was IFN-γ inductive and IL-4 non-inductive HTL cell epitopes and had population coverage corresponding to MHC molecular alleles associated with T-cell phenotype. The multivalent enterovirus vaccine was constructed to connect the 50 s ribosomal protein L7/L12 adjuvant and candidate epitopes sequentially through appropriate linkers. Then, the antigenic, allergen and physical properties of the vaccine were evaluated, followed by a secondary structure analysis and tertiary structure modeling, disulfide engineering, refinement and validation. Moreover, the conformational B cell epitope of the vaccine was analyzed. The stability of the TLR4/MD2/Vaccine complex and details at atomic level were investigated by docking and molecular dynamics simulation. Finally, in silico immune simulation and in vivo immune experiments were done. This study provides a high cost-effective method of designing a multivalent enterovirus vaccine protect against a wide range of enterovirus pathogens.

1. Introduction

Enteroviruses are non-enveloped single-stranded positive-strand RNA viruses that belong to the *Picornavirus* family of the genus, *Enteroviruses*. There are 13 species of enteroviruses and 7 of them are human pathogens, while more than 250 serotypes have been identified, including Poliovirus, Coxsackievirus group A (CV-A, type 1–22 and type 24), Coxsackievirus group B (CV-B, type 1–6), Enterovirus (EV, type 68–71), Echovirus and Rhinovirus [1,2]. Enteroviruses cause self-limiting and mild neonatal disease that are mainly caused by type A Enteroviruses but are sometimes caused by type B Enteroviruses. Clinical manifestations include fever, blisters on the hands, feet, hips and in the mouth (HFMD), in addition, several enterovirus species may cause serious and life-threatening cardiopulmonary diseases and neurological complications, such as aseptic meningitis, neonatal sepsis-like disease, encephalitis, acute flaccid paralysis, non-specific febrile illness, herpangina, pleurodynia, pericarditis and myocarditis [3]. CV-B3 is the main pathogen that causes viral myocarditis, which has epidemic risk in China [4]. Based on epidemiological research, Enterovirus A71 (EV-A71), Coxsackievirus A16 (CV-A16) and Coxsackievirus A6(CV-A6) accounting for the most cases of HFMD [5]. Molecular epidemiological surveillance in Asian countries show that CV-A6, CV-A10 and CV-A16 are the most common coxsackie viruses that cause HFMD outbreaks among children [6–8]. The co-circulation of these viruses increase the risk of co-infection and genetic recombination which has resulted in public health problems [2,9].

Currently, three inactivated EV-A71 vaccines are marketed in China [10–12]. Although these vaccines have been quite successful in inducing a neutralization response against EV-A71 infection, in

* Corresponding authors at: Center of Pathogen Biology and Immunology, Department of Microbiology and Immunology, Shantou University Medical College, Shantou 505041, Guangdong, China.
E-mail addresses: gefeiwang@stu.edu.cn (G. Wang), 07rli1@stu.edu.cn (R. Li).

https://doi.org/10.1016/j.vaccine.2020.03.023
0264-410X/

20% of subjects, it was found that the NHRI EV71 vaccine based on the B4 subgenotype only triggered a weak neutralization response against CV-A16, while the EV-A71 vaccine based on the C4 serotype did not show any neutralization response against CV-A16, making them unsuitable for the prevention HFMD caused by CV-A16 and other enteroviruses, even the genomic sequence of EV-A71 is similar to that of CV-A16 [10,13]. A monovalent formalin-inactivated CV-A16 vaccines have been shown to induce significant neutralizing antibody responses against different subtypes of CV-A16 in neonatal mouse models and are able to provide protection against lethal attacks, but not against EV-A71 [14]. Therefore, the monovalent vaccine can only prevent against a small number of HFMD cases and a multivalent vaccine containing CV-As is required to achieve broader protection against HFMD. Designing a multivalent enterovirus vaccine that can induce immune resistance against multiple enteroviruses, based on conservative epitopes, is an ideal strategy. In our study, we design a multivalent vaccine against major epidemic outbreak enterovirus based on immune-information and the immunogenicity of vaccine was evaluated in silico and in vivo. A schematic representation of the enterovirus multivalent epitopes subunit vaccine candidate designing process is shown in Fig. 1.The foremost objective is to produce humoral and cell-mediated immune responses to a wide range of enteroviral infections.

2. Method

2.1. Sequence data retrieval of multivalent enterovirus vaccine

We chose EV-A71 C4 strain (AJR21495.1), CV-A16 (ARU09511.1), CV-A6 (AXH81620.1), CV-A10 (ARU09505.1), CV-B3 (AAA42931.1) as vaccine candidates, using the NCBI Protein database (https://www.ncbi.nlm.nih.gov/protein). 957 EV-A71 protein sequences, 403 protein CV-A6 sequences, 189 CV-A16 protein sequences, 83 CV-A10 protein sequences and 67 CV-B3 protein sequences were used as templates for the epitope conservancy analysis. The 50S ribosomal protein L7/L12, with 130 amino acid residues, that was used as an adjuvant, was extracted through UniProt. All protein sequences were collected in FASTA format.

2.2. Epitope prediction

ABCPreds (http://crdd.osdd.net/raghava/abcpred/) and BCPreds (http://ailab.ist.psu.edu/bcpred/) were used to predict the B-linear epitopes. ABCPred is based on recurrent neural networks with an accuracy of 65.93%, default threshold of 0.51 and window length of 16 [15]. BCPred used in the kernel method allow the user to select from among three prediction methods: (i) AAP method (amino acid pair antigenicity; AUC = 0.7); (ii) BCPred (AUC = 0.758); (iii) FBCPred.

The IEDB Sever (http://www.iedb.org/) and RANKPEP Sever (http://imed.med.ucm.es/Tools/rankpep.html) were used to predict the MHC-Ⅱ banding epitope [16,17]. IEDB default parameter settings and a reference set that can reach 99% of the coverage of the minimum allele in HLA allele was used [18]. The results were ranked by percentile and IC50. IC50 < 50 nm indicates high affinity, while IC50 < 500 nm and IC50 < 5000 nm indicates intermediate affinity and low affinity, respectively. RANKPEP used Position Specific Scoring Matrices (PSSMs) or profiles from a set of aligned peptides known to bind to a given MHC molecule as the predictor of MHC-peptide binding, focusing on predicting conservative epitopes and avoiding immune escape caused by mutations [17]. The default parameter was used to predict the score of the 9-mer MHC-II binding epitope with a 4–6% binding threshold, while the binding potential of epitopes to MHCII was evaluated using EpiTOP (http://www.pharmfac.net/EpiTOP/index.php) [19], a chemometric tool for MHC II binding prediction. The parameters were set to default values. Using IFNepitope (http://crdd.osdd.net/raghava/ifnepitope/) and IL4pred (http://crdd.osdd.net/raghava/il4pred/), the IFN-γ inducing and the non IL4-inducing epitopes were predicted. IFNepitope uses the motif and support vector machine (SVM) to predict an epitope, based on the set of IFN-γ inducing and non MHC-Ⅱ inducing epitopes [20]. IL4pred is a predictive model based on three dataset trainings, that calculate the IL-4

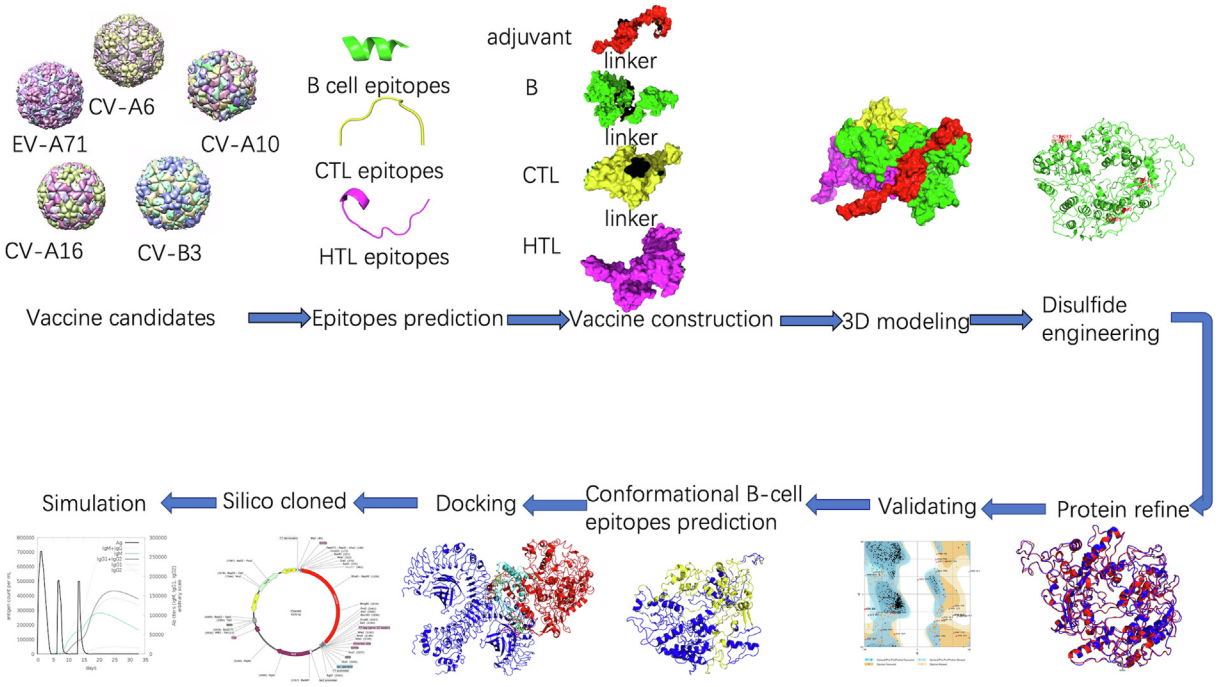

Fig. 1. Schematic representation of the enterovirus multivalent epitopes subunit vaccine candidate designing process using B-cell, CTL and HTL epitopes, followed by 3D modeling, disulfide engineering, protein refining, conformational B-cell epitopes prediction, molecular docking, in silico cloning and simulation.

induction ability of each peptide using default parameters [21]. In our study, the non-IL-4 epitopes were selected as the target epitopes.

MHC I binding to the CTL epitope was predicted using the NetMHCpan 4.0 server (http://imed.med.ucm.es/Tools/rankpep.html), IEDB server (http://tools.iedb.org/mhci/), Rankpep server (http://imed.med.ucm.es/Tools/rankpep.html), CTLpred (http://crdd.osdd.net/raghava/ctlpred/) and NetCTL server 1.2 (http://www.cbs.dtu.dk/services/NetCTL/). The parameters of all server HLA alleles were chosen to reach 97% population coverage [22]. The NetMHCpan 4.0 server predicts the binding of peptides to any MHC molecule on a known sequence using artificial neural networks (ANNs) [22]. The MHC allele and peptide length were set to the HLA supertype representative and 9-mer peptides, respectively, while other parameters were set at default values. The server divides the epitopes into strong and weak conjugates by calculating the level of binding of the peptide. In this study, only strong combinations were selected for further analyses. The IEDB server is another online server that uses the recommended consensus methods of ANN, SMM, and CombLib [23]. Rankpep predicts the highest score of the MHC-I binding peptide at a 2–3% binding threshold using PSSM [17]. CTLpred uses the pattern of T cell epitopes instead of MHC binders to predict CTL epitopes using elegant machine learning techniques, such as Support Vector Machine (SVM) and Artificial Neural Networks [24]. NetCTL is a web based tool for CTL epitopes prediction for any given protein [25], which uses a prediction method that integrates the prediction of MHC class I binding peptides, proteasomal C-terminal cleavage, and TAP (Transporter Associated with Antigen Processing) transport efficiency. The threshold value for epitope identification was set as 0.75 (default score) for the prediction of CTL epitopes. All predicted epitopes were tested for immunogenicity using IEDB (http://tools.iedb.org/immunogenicity/) and non-toxicity was confirmed based on physical and chemical properties by ToxinPred (https://webs.iiitd.edu.in/raghava/toxinpred/design.php) [26,27]. A higher level of reliability in epitope prediction can be achieved by using multiple tools instead of using only a single tool.

2.3. Identification of protective epitopes

In order to select appropriate epitopes for further analysis, the verified linear epitopes can be used as the preferred reference for epitopes of multivalent enteroviruses. Then, the B cell epitopes, HTL epitopes, and CTL epitopes generated by the servers were compared to identify of the best segment with high overlap that make epitopes have ability to induce humoral and cellular immune responses. As the identification of each epitope is performed by several servers, the epitope obtained may induce a specific immune response. The MHC I conjugate and the overlapping region between the CTL and B cell epitopes were used to select a potential epitope, while the IEDB server (http://tools.immuneepitope.org/mhcii/) was used to obtain the IEDB score of the best conjugate [16].

2.4. Conservancy and population coverage analysis of T-cell (HTL & CTL) epitopes

Conservative levels of viral serotypes were assessed using the IEDB Analysis Resource's Epitope Conservancy Analysis server (http://tools.iedb.org/conservancy/) [28]. Conservation of the epitopes was calculated based on sequence alignment between the identified epitopes and the five viral serotypes. The Analysis type and Sequence identity threshold were set to "linear" and "100%", while default values were used for other parameters. IEDB was used to evaluate the population coverage of the predicted T cell epitopes (MHC I and II), which is important for the development of the global vaccine candidate [29]. We analyzed the world and enteroviral outbreak areas of northeast Asia and East Asia, China's population data sets, and the MHC Ⅰ and MHC Ⅱ combined analysis of population coverage.

2.5. Vaccine construction

Based on the epitopes obtained from the above immunological informatics analysis, and ensure obtained that protein with good stability, domain orientation and folding rate [30], we used KK, AAY and GPGPG linkers to connect together B cell epitopes, as well as HTL and CTL epitopes. Moreover, the 50S ribosomal protein L7/L12 was added to the N-terminal using the EAAAK linker. At the site of host infection, the 50S ribosomal protein L7/L12 of *Mycobacterium tuberculosis* Rv0652 is able to induce dendritic cells (DC) and naïve T cells to mature and mediate the production of inflammatory cytokines and enhance cellular immunity by interacting with TLR4 [31].

2.6. Antigenicity, allergenicity, solubility and secondary structure prediction

Vexigen v2.0 (http://www.ddg-pharmfac.net/vaxijen/VaxiJen/VaxiJen.html) and ANTIGENpro (http://scratch.proteomics.ics.uci.edu/) were used to predict the antigenicity of constructed multi-epitope vaccines [32,33]. Antigenicity prediction is based on an alignment-independent algorithm. It depicts the antigenicity of the protein based solely on the physicochemical properties of the input vaccine sequence, whose accuracy ranges from 70 to 89% in various organisms [32]. The AllerTop server (http://www.pharmfac.net/allertop/) based on Auto cross-covariance (ACC) of transformation of the protein sequence into uniform equal-length vectors, was used to predict the allergenic nature of the final vaccine construct. Compared with the other severs, the prediction sensitivity of AllerTop can reach a high level of up to 94% [34]. SOLpro (http://scratch.proteomics.ics.uci.edu/) is used to predict the solubility of the vaccine proteins constructed, which in turn predicts the propensity of a protein to be soluble upon overexpression in *E. coli,* using a two-stage SVM architecture based on multiple representations of the primary sequence [35]. The physicochemical properties of the vaccine, including molecular weight, isoelectric point (PI), half-life, and stability, were predicted using the ExPASy database server (https://web.expasy.org/protparam/). The "N-terminal rule" was used to calculate the half-life, that is, the half-life of the protein in the body, which is determined by the N-terminal amino acid residues. GRAVY is obtained by dividing the total amino acid hydrophilicity by the number of amino acids in the amino acid, which is a measure of the hydrophilicity of the protein [36]. Secondary structure of the protein was predicted by RaptorX (http://raptorx.uchicago.edu/StructPredV2/predict/) and PSIPRED 4.0 (http://bioinf.cs.ucl.ac.uk/psipredtest) [37].

2.7. Tertiary structure prediction

The tertiary structure of the final protein vaccine was ascertained using the I-TASSER

online server (https://zhanglab.ccmb.med.umich.edu/I-TASSER/). The I-TASSER server is an online platform for high-resolution modeling of proteins and its functions, which involves four consecutive steps [38]. The PyMOL program was used for visualization of the 3D models.

2.8. Vaccine protein disulfide engineering

Disulfide engineering has been proven to help improve protein stability and contribute to the study of protein dynamics and

interactions [39]. In the 3D model, it is necessary to design the disulfide bond of the predicted protein in a manner that improves the stability of the protein. The Disulfide by Design2.0 server (http://cptweb.cpt.wayne.edu/DbD2/index.php) was used to design the disulfide bonds of the protein. By uploading the protein model, the residue pair is used to search for a suitable design of a disulfide bond. Using the create mutate function of the Design 2.0 server, the high B-factor residues were selected to mutate them with cysteine residue.

2.9. Tertiary structure refinement and validation

GalaxyRefine (http://galaxy.seoklab.org/cgi-bin/submit.cgi?type=REFINE) was used to refine the tertiary structure [40]. In order to verify the quality of the tertiary structure model, we used the RAMPAGE online server (http://mordred.bioc.cam.ac.uk/~rapper/rampage.php) and ProSA-web (https://prosa.services.came.sbg.ac.at/prosa.php) to analyze the model. ProSA-web computes the interaction energy of each residue with the rest of the protein to determine if it achieves a certain energy criterion. ProSA calculates an overall quality score for a specific input structure. If the score is outside of characteristic range for native proteins, the structure probably contains errors [41]. Ramachandran plot involves the prediction of the energetically disallowed and allowed dihedral psi (ψ) and phi (Φ) of amino acid residues, which are calculated based on the Van der Waals radius of side chain atoms [42].

2.10. Conformational B-cell epitope prediction

Conformational B-cell epitopes of the vaccine protein tertiary structure were predicted using DiscoTope 2.0 (http://www.cbs.dtu.dk/services/DiscoTope/), which calculates surface accessibility (estimated in terms of contacts numbers) and a novel epitope propensity amino acid score. The final score is calculated by combining the propensity score of residues in spatial proximity with the contact numbers [43]. A default threshold of −3.7 was used with sensitivity and specificity values of 0.47 and 0.75, respectively.

2.11. Protein-protein docking

ClusPro 2.0 (https://cluspro.bu.edu/login.php) was used to predict the interaction between protein molecules [44], TLR-4/MD2 (PDB ID:4G8A) was used as the receptor, and the refined protein vaccine was used as the ligand. Then, removed water and other small molecules from TLR-4/MD2 by pyMOL. The docking complexes produced by the server had adequate free energy for dissolving and electrostatic interactions. LigPLot+ was used to determine the amino acid residues of the vaccine ligand, TLR-4 receptor with hydrogen bonds and hydrophobic effect [45]. Molecular dynamics simulation was performed by GROMACS 2019.4-lcc, and the Amber force field was selected. Equilibration steps by energy minimization, NVT and NPT for a time duration of 10,000 ps, 500 ps and 1000 ps, respectively. MD production was also performed for 15 ns. Finally, the root mean square deviation (RMSD) for backbone and root mean square fluctuation (RMSF) for side chain was determined and the binding free energy for the association of TLR4/MD2/Vaccine complex was calculated use the MM-PBSA, which performed by Amber.

2.12. A5V codon adaptation, expression and purification

The multi-epitope vaccine protein sequence was reverse translated using SnapGene software. We choose bacterial, archaeal and plant plastids as genetic code, and reverse translated using *Escherichia coli* and probable codons that were chosen based on frequency distribution. Later on, in order to express the designed protein vaccine efficiently and stably in the prokaryotic expression system (*E. coli* BL21), the protein vaccine DNA was cloned into a pET28a (+) vector using in silico cloning. The method of A5V expression and purification is described in Supplement method.

2.13. A5V immunogenicity evaluated in silico and in vivo

The immunogenicity and immune response of the multi-epitope vaccine were conducted by the C-ImmSim server (http://150.146.2.1/C-IMMSIM/index.php) which predicted immune epitopes based on an agent-based model that uses a position-specific scoring matrix (PSSM) and predicted immune interactions by used machine learning techniques [46]. In this experiment, the following set of MHC alleles have been used, HLA A*11:01, HLA A*31:01, HLA B*35:01, HLA B*53:01, HLA DRB5*01:01, HLA DRB1*09:01 in which based on the population coverage. Three injections were given at intervals of one week according to the typical immunization process. All simulation parameters were set at default with time steps set at 1, 20, and 40 (each time step is 8 h and time step 1 is injection at time 0). The actual AA sequence of vaccine used as an antigenic molecule. In vivo experiment, the method of A5V immunogenicity evaluated in vivo is described in Supplement method.

3. Result

3.1. Epitope prediction

B cell epitopes play an important role in humoral immunity, preventing viruses from invading the body. In the selection of epitopes, we gave priority to previously reported epitopes. In the prediction of epitopes based on the neural algorithm, a variety of algorithms were used to predict the epitopes, and at the same time improve accuracy. There are some linear epitopes that have been proven to induce neutralizing antibodies, such as SP70, SP55, SP28, PEP27, VP1-15, VP2 (aa141-155s), VP4 N20, PEP23, K1, K2, K3 of EV-A71; and PEP32, PEP37, PEP55, PEP63, PEP71, PEP91 of CV-A16, P42 and P59 of CV-A6. For the HTL epitopes, IFN-γ is the signature cytokine of both the innate and adaptive immune system, which elicits antiviral, immune regulatory, as well as antitumor activities. The release of IFN-γ is a major defense mechanism of Th1 response that is critical for the control of intracellular pathogens, such as *Mycobacterium tuberculosis*, while IL-4 is a major mechanism of Th2 response. High expression of IL-4 would inhibit IFN-γ production and affect the function of TH1 cells to clear viral infection. In our study, IFN-γ and non-IL-4 inducing epitopes were identified using the IFN epitope server and IL4pred, respectively. All the epitope candidates were IFN-γ inducing and non-IL-4 inducing, in order that the selected epitopes have the ability to induce a Th1 cell mediated immune response. The overlapping regions of the same type of epitopes predicted by different servers were selected as candidate epitopes, and the ToxinPred server and IEDB were used to analyze the toxicity and conservativeness, respectively, of these epitopes. Finally, 23 B cell epitopes (Table 1), 13 HTL epitopes (Table 2) and 15 CTL epitopes (Table 3) that are non-toxic and highly conservative were identified. Conservative results show that all candidate epitopes of the five vaccine candidate templates are highly similar, which suggests corresponding cross-immune protection.

A given epitope can only induce a response in individuals that express the corresponding specific MHC molecule. Selecting multiple peptides with different HLA binding specificities will afford for increased coverage of the patient population that is targeted by epitope-based vaccines or diagnostics. Moreover, 91.45%, 95.42%

Table 1
Linear B-cell epitope prediction for the EV-A71, CV-A6, CV-A10, CV-A16, CV-B3 protein sequences, as well as toxin prediction and conservancy analysis of each epitope.

Name	Sequence	Start position	Toxin prediction	Percent of protein sequence matches at identity ≤100%	Minimum identity
EV-A71-1	EDTHPPYKQTQPGADG	211	Non-Toxin	29.13% (495/1699)	31.25%
EV-A71-2	FHPTPCIHIPGEVRNL	351	Non-Toxin	55.39% (941/1699)	31.25%
EV-A71-3	QAAEIGASSNASDESM	613	Non-Toxin	41.85% (711/1699)	31.25%
EV-A71-4	TFVACTPTGEVVPQLL	701	Non-Toxin	45.73% (777/1699)	31.25%
EV-A71-5	VPPGAPKPDSRESLAW	721	Non-Toxin	49.68% (844/1699)	31.25%
EV-A71-6	PTFGEHKQEKDLEYGA	774	Non-Toxin	55.56% (944/1699)	25.00%
EV-A71-7	KHVRAWIPRPMRNQNY	821	Non-Toxin	52.68% (895/1699)	25.00%
EV-A71-8	AVTQGFPTELKPGTNQ	320	Non-Toxin	42.50% (722/1699)	37.50%
CV-A16-1	SIITMPTTGTQNTDGY	656	Non-Toxin	10.12% (172/1699)	31.25%
CV-A16-2	WQTATNPSVFVKMTDP	736	Non-Toxin	10.65% (181/1699)	37.50%
CV-A16-3	FGEHLQANDLDYGQCP	776	Non-Toxin	10.30% (175/1699)	31.25%
CV-A16-4	YDGYPTFGEHLQANDL	770	Non-Toxin	10.36% (176/1699)	31.25%
CV-A16-5	PYLFKTNPNYKGNDIK	835	Non-Toxin	10.30% (175/1699)	31.25%
CV-A6-1	PTFGEHKQATNLQYGQ	769	Non-Toxin	21.95% (373/1699)	25.00%
CV-A6-2	ASITTTDYEGGVPANP	851	Non-Toxin	20.54% (349/1699)	25.00%
CV-A10-1	GCHGSPWAWIKAKTAS	1086	Non-Toxin	85.46% (1452/1699)	31.25%
CV-A10-2	PVCLIIRGSPGTGKSL	1233	Non-Toxin	94.64% (1608/1699)	68.75%
CV-A10-3	YNFPTKAGQCGGVVTS	1686	Non-Toxin	88.23% (1499/1699)	31.25%
CV-A10-4	TNASNIIVPTVSDSDA	1333	Non-Toxin	81.81% (1390/1699)	37.50%
CV-B3-1	RMLMYNFPTRAGQCGG	1674	Non-Toxin	3.94% (67/1699)	31.25%
CV-B3-2	FHQGCLLVVCVPEAEM	186	Non-Toxin	3.88% (66/1699)	43.75%
CV-B3-3	YFVRGGMPSGCSGTSI	2004	Non-Toxin	3.88% (66/1699)	37.50%
CV-B3-4	YSLPPDPDHFDGYKQQ	1255	Non-Toxin	99.12% (1684/1699)	37.50%

Table 2
Helper T-lymphocyte specific epitope prediction for the EV-A71, CV-A6, CV-A10, CV-A16, CV-B3 protein sequences, as well as IFN-γ and IL-4 inducer prediction and conservancy analysis of each HTL epitope.

Name	Sequence	Allele	Start position	Percentile rank	Smm_ic50	IFN-γ inducer	IL-4 inducer	Percent of protein sequence matches at identity ≤100%	Minimum identity
EV-A71-1	RALTQALPAPTGQNT	HLA-DRB1*09:01	583	0.6	109	POSITIVE	Non inducer	16.07% (273/1699)	33.33%
EV-A71-2	PASAYQWFYDGYPTF	HLA-DRB3*01:01	762	0.38	116	POSITIVE	Non inducer	71.92% (1222/1699)	33.33%
EV-A71-3	VRIYMRMKHVRAWIP	HLA-DRB1*11:01 HLA-DRB3*02:02	814	0.11	48	POSITIVE	Non inducer	35.61% (605/1699)	26.67%
CV-A16-1	WDFGLQSSVTLVVPW	HLA-DRB1*04:01	480	0.77	51	POSITIVE	Non inducer	9.77% (166/1699)	33.33%
CV-A16-2	TAVQVLPTAANTEAS	HLA-DRB1*08:02	586	0.32	295	POSITIVE	Non inducer	0.12% (2/1699)	33.33%
CV-A16-3	QGHFTMLGVRDRLAI	HLA-DRB5*01:01	1570	0.99	134	POSITIVE	Non inducer	14.54% (247/1699)	33.33%
CV-A16-4	PVWFRALEVVLREIG	HLA-DRB5*01:01 HLA-DPA1*02:01 /DPB1*14:01	1974	0.95	58	POSITIVE	Non inducer	18.36% (312/1699)	33.33%
CV-A6	RPILRTATVQGPSLD	HLA-DRB1*08:02	1547	0.58	409	POSITIVE	Non inducer	0.82% (14/1699)	33.33%
CV-A10-1	SPVWFRALEMVLRDI	HLA-DRB5*01:01 HLA-DPA1*02:01 /DPB1*14:01	1973	0.57	–	POSITIVE	Non inducer	4.36% (74/1699)	33.33%
CV-A10-2	SAYQWFYDGYPTFGQ	HLA-DRB3*01:01	762	0.33	119	POSITIVE	Non inducer	4.94% (84/1699)	26.67%
CV-B3-1	WINLRTNNSATIVMP	HLA-DRB1*13:02	260	0.02	6	POSITIVE	Non inducer	3.77% (64/1699)	33.33%
CV-B3-2	PGYSSVFSRTLLGEI	HLA-DRB1*07:01 HLA-DRB1*09:01	421	0.9	12	POSITIVE	Non inducer	3.94% (67/1699)	33.33%
CV-B3-3'	AEWVLTPRQAAQLRR	HLA-DRB1*11:01	658	0.9	45	POSITIVE	Non inducer	0.88% (15/1699)	33.33%

and 91.32% of the population was covered in Northeast Asia, East Asia and China, respectively, which together make up the main endemic zone of enterovirus (Table 4). The allelic frequency data confirm that the selected T-cell epitopes have global distribution characteristics that make them suitable for use in designing the candidate protein vaccine.

The IEDB population coverage server was used to evaluate the population coverage of the 30 identified HTL and CTL epitopes. A given epitope can only induce a response in individuals that express the corresponding specific MHC molecule. Selecting multiple peptides with different HLA binding specificities will afford for increased coverage of the patient population that is targeted by

Table 3
Cytotoxic T-lymphocyte specific epitope prediction, toxin prediction, immunogenicity and conservancy analysis for the EV-A71, CV-A6, CV-A10, CV-A16, CV-B3 protein sequences.

Name	Sequence	Allele	Start position	Immunogenicity	Toxin prediction	Percent of protein sequence matches at identity ≤100%	Minimum identity
EV-A71-1	SMINNIIIR	HLA-A*31:01 HLA-A*68:01 HLA-A*11:01 HLA-A*03:01	2030	0.34575	Non-Toxin	97.53% (1657/1699)	44.44%
EV-A71-2	ISKFIDWLK	HLA-A*11:01 HLA-A*68:01 HLA-A*30:01 HLA-A*31:01	1136	0.37874	Non-Toxin	80.46% (1367/1699)	44.44%
EV-A71-3	EAANIIVGY	HLA-A*26:01 HLA-A*68:01 HLA-B*35:01 HLA-B*53:01	96	0.31571	Non-Toxin	56.09% (953/1699)	55.56%
CV-A16-1	REQGWIIPE	HLA-B*40:01 HLA-B*35:01	1478	0.44332	Non-Toxin	22.60% (384/1699)	33.33%
CV-A16-2	EVTWENATF	HLA-A*26:01	2097	0.3826	Non-Toxin	33.78% (574/1699)	55.56%
CV-A16-3	YVNWDIDLM	HLA-A*26:01 HLA-B*35:01	671	0.37991	Non-Toxin	10.71% (182/1699)	33.33%
CV-A6-1	MINNIIIRA	HLA-A*31:01 HLA-A*68:01	2038	0.38883	Non-Toxin	44.97% (764/1699)	44.44%
CV-A6-2	ATGIVTIWY	HLA-A*01:01 HLA-A*30:02	513	0.4634	Non-Toxin	23.37% (397/1699)	44.44%
CV-A6-3	LSYGEWPEY	HLA-A*01:01 HLA-A*30:02 HLA-B*35:01	102	0.38805	Non-Toxin	23.43% (398/1699)	44.44%
CV-A10-1	YATWDIDIM	HLA-B*35:01 HLA-B*53:01	669	0.47885	Non-Toxin	5.00% (85/1699)	33.33%
CV-A10-2	LAYGEWPEY	HLA-A*30:02 HLA-B*35:01 HLA-B*53:01	102	0.38805	Non-Toxin	5.00% (85/1699)	44.44%
CV-A10-3	VEDIIHDAL	HLA-B*40:01	568	0.34275	Non-Toxin	5.00% (85/1699)	44.44%
CV-B3-1	KSTIRIYFK	HLA-A*03:01 HLA-A*11:01 HLA-A*30:01 HLA-A*31:01 HLA-A*68:02	800	0.38748	Non-Toxin	3.94% (67/1699)	44.44%
CV-B3-2	VAGIIYIIY	HLA-B*35:01 HLA-A*30:02 HLA-B*57:01	1503	0.46112	Non-Toxin	3.83% (65/1699)	33.33%
CV-B3-3	TSPGWWWKL	HLA-A*24:02 HLA-A*32:01 HLA-A*26:01 HLA-A*23:01	143	0.51565	Non-Toxin	3.77% (64/1699)	44.44%

Table 4
Population coverage calculation of the HTL epitope and CTL epitope specific alleles.

Population/area	MHC class	Coverage[a]	Average_hit[b]	PC90[c]
World	Combined	95.53%	5.42	1.93
Northeast Asia	Combined	91.45%	4.23	1.17
East Asia	Combined	95.42%	5.24	1.51
China	Combined	91.32%	4.21	1.15

[a] Projected population coverage.
[b] Average number of epitope hits/HLA combinations recognized by the population.
[c] Minimum number of epitope hits/HLA combinations recognized by 90% of the population.

epitope-based vaccines or diagnostics. Moreover, 91.45%, 95.42% and 91.32% of the population was covered in Northeast Asia, East Asia and China, respectively, which together make up the main endemic zone of enterovirus (Table 4). The allelic frequency data confirm that the selected T-cell epitopes have global distribution characteristics that make them suitable for use in designing the candidate protein vaccine.

3.2. Antigenicity, allergenicity, solubility and physicochemical parameter evaluation and the secondary structure of the vaccine

The constructed vaccine has 987 amino acid residues, and its molecular weight and isoelectric point are 107 kDa and 9.17, respectively. Its half-life is 30 h in the reticular erythrocytes of mammals, more than 20 h in yeast, and more than 10 h in *E. coli*. Its instability index value is 29.45 < 40, indicating that the protein is stable. The aliphatic chains index and the GRAVY (Grand average of hydropathicity) of the protein are 71.07 and −0.348, respectively. The aliphatic chains index of the protein structure indicates

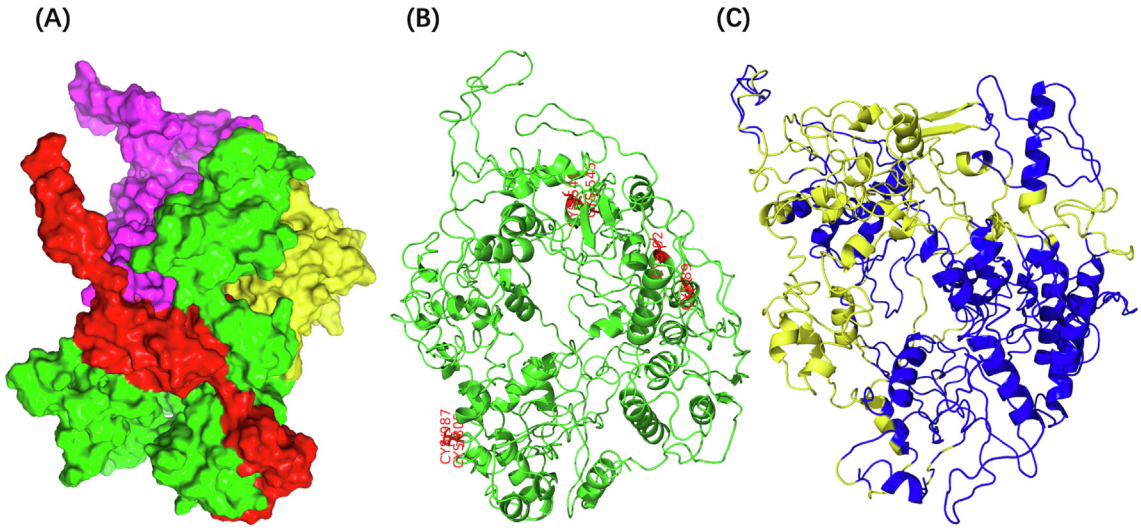

Fig. 2. Tertiary structure prediction, disulfide engineering and Conformational B-cell epitopes validation. (A) The model chosen through tertiary structure development for the multivalent enterovirus epitopes subunit vaccine**.** Red color indicates adjuvants, green color indicates B cell epitopes, yellow color indicates CTL epitopes, while violet color indicates HTL epitopes. (B) Disulfide engineering of protein vaccine. (C) Conformational B-cell epitopes of the constructed protein vaccine. Conformational B-cell epitopes are colored yellow. (For interpretation of the references to color in this figure legend, the reader is referred to the web version of this article.)

the thermostability of the protein. The GRAVY value indicates the average hydrophobicity, while the greater negative value indicates hydrophilicity. The results of the Vexigen 2.0 and ANTIGEN analyses show that the multivalent epitopes vaccine that was designed is potentially antigenic in nature, while the AllerTOP v2.0 server defined the protein as non-allergenic. The secondary structure of vaccine was found to consist of 27% alpha helixes, 11% extended strands and 60% random coils. Solvent accessibility (ACC) found that 26% of the amino acid residues were buried, 25% had medium exposure, while 48% were fully exposed (Supplementary Fig. 1).

3.3. Tertiary structure prediction

The primary tertiary structure model of the multivalent enterovirus epitopes subunit vaccine was generated using the I-TASSER program. The C-score of the top 5 predicted models were −0.74, −0.75, −1.76, −4.16 and −4.31, with a higher C score indicating higher model confidence. In addition, the best template modeling (TM) score and the root-mean-square deviation (RMSD) for this model were 0.62 ± 0.14 and 10.6 ± 4.6 Å, respectively. We selected model 1 as the final tertiary structure model (Fig. 2A) selected for further designing.

3.4. Disulfide engineering of the protein vaccine

Disulfide engineering can improve the structural stability of many extracellular secretion proteins. Suitable disulfide engineering can reduce conformational entropy and improve free energy of the degenerated state. The 3D structure of the protein vaccine analysis shows 91 pairs potential disulfide bonds. 3 pairs of disul-

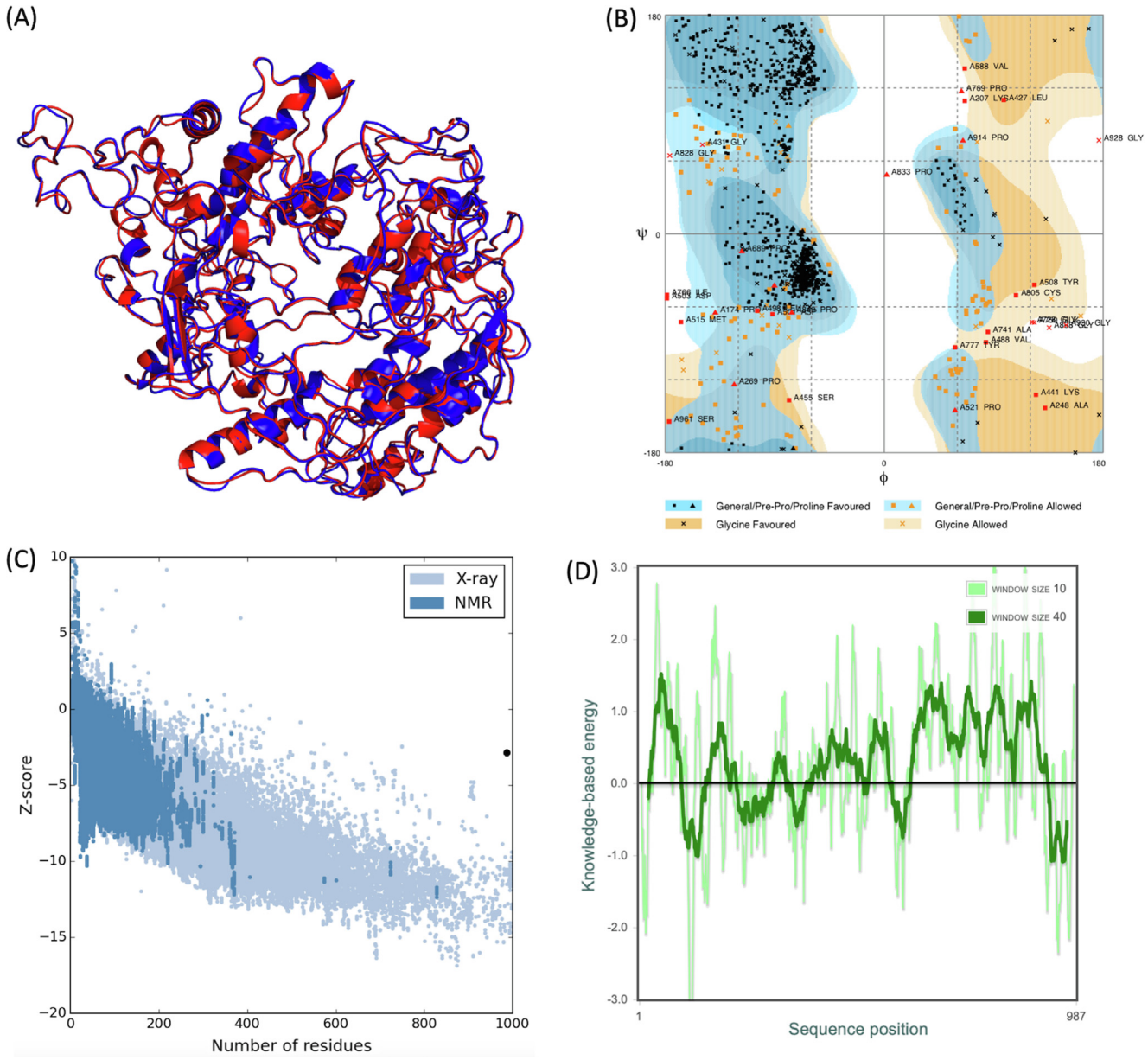

Fig. 3. Tertiary structure model refinement and validation. (A) Comparison between tertiary protein structures. The initial and refined models are colored blue and red, respectively; (B) Ramachandran plot shows the presence of amino acid residues in favored, allowed and outlier regions; (C) ProSA-SEB plot Z-Score of the best model was found to be −2.84, which is in the range of conformational native proteins; (D) The plot shows local model quality by plotting energy as a function of amino acid sequence position. (For interpretation of the references to color in this figure legend, the reader is referred to the web version of this article.)

fide bridges were selected based on their high ΣB-factor values of 21.48, 19.38 and 19.66. In the spanning region of high mobility these residues were substituted in place of GLY-89-GLU-92; GLU-541-THR-545; VAL-805-ILE-987 and mutated to CYS89-CYS92; CYS541-CYS545 and CYS805-CYS987. The effect of a given disulfide on the overall stability of a protein appears to be dependent on multiple factors. The B-factor analysis can assist in the identification of potential disulfides that may confer an improvement in stability. Furthermore, these mutations were created using the visualization program, PyMOL, and the mutant form was generated to increase the stability of the designed vaccine (Fig. 2B).

3.5. Tertiary structure model refinement and validation

The GalaxyRefine program was applied to refine the disulfide engineered model structure, and 5 refined models built. After investigating the models using Ramachandran plot, refine model 3 was chosen as the best, based on various parameters, including GDT-HA (0.8880), RMSD (0.571), Molprobity (2.438), Clash score (17.2), poor rotamers (0.8) and Ramachandran plot (82.3). Comparison between the initial and refined model is shown in Fig. 3A. Validation of the refined tertiary structure model using Ramachandran plot indicted that 821 (83.4%), 131 (13.3%) and 33 (3.4%) of residues are located in favored, allowed and outlier regions, respectively, in the refined model (Fig. 3B); while 595 (60.4%), 258 (26.2%) and 132 (13.4%) of residues were located in favored, allowed and outlier regions, respectively, in the initial model. ProSA-web (Protein structure analysis) has shown that the Z-score of −2.84 for the protein vaccine lies inside the score range that is common for native proteins of a comparable size (Fig. 3C). The plot shows local model quality by plotting energy as a function of amino acid sequence position (Fig. 3D). In general, positive values indicate problematic or erroneous parts of the input structure. The results indicate the accuracy of the polyvalent epitope protein structure of the enterovirus based on homology modeling that was satisfactory for use in further analyses.

3.6. Predicted conformational B-cell epitopes

In order to confirm B-cell induction by the designed vaccine, the conformational B-cell epitopes were predicted using DisoTope 2.0. A total of 380 B-cell epitope residues were identified out of 987 total residues (Fig. 2C and Supplement data 2).

3.7. Molecular docking and MD analysis of the subunit vaccine with TLR-4 immune receptor

Cluspro uses the rigid docking method of exhaustive sampling to locate the closest primitive interaction structure. Cluspro was used to analyze the ability of the vaccine to bind to the TLR-4 immune receptor (PDB: 4G8A) under four different energy modes. Each energy mode resulted in 30 clusters, all of which had their own weight scores. Referring to known structures of the TLR4-MD-LPS complex, TLR4 cannot bind to LPS alone, but also requires the participation of MD2 co-receptors. The extracellular domain of MD2 and TLR4 directly bind to LPS. Under the cluster of Van der Waals force and electrostatic force energy model, cluster 15 was found to be the closest cluster to that of the reference complex structure (Fig. 4A), which showed complex interactions between receptors and ligands involving 13 members at the 9 Å C-alpha RMSD radius and its center. The lowest energies of the weighted fractions were −246.0 and −246.0, respectively. It is possible to activate antiviral immunity through interaction with TLR-4. LigPLot+ was used to determine the key amino acid residues involved in the interaction between the vaccine and TLR-4. A total of 17 amino acid residues of the vaccine were found to interact with

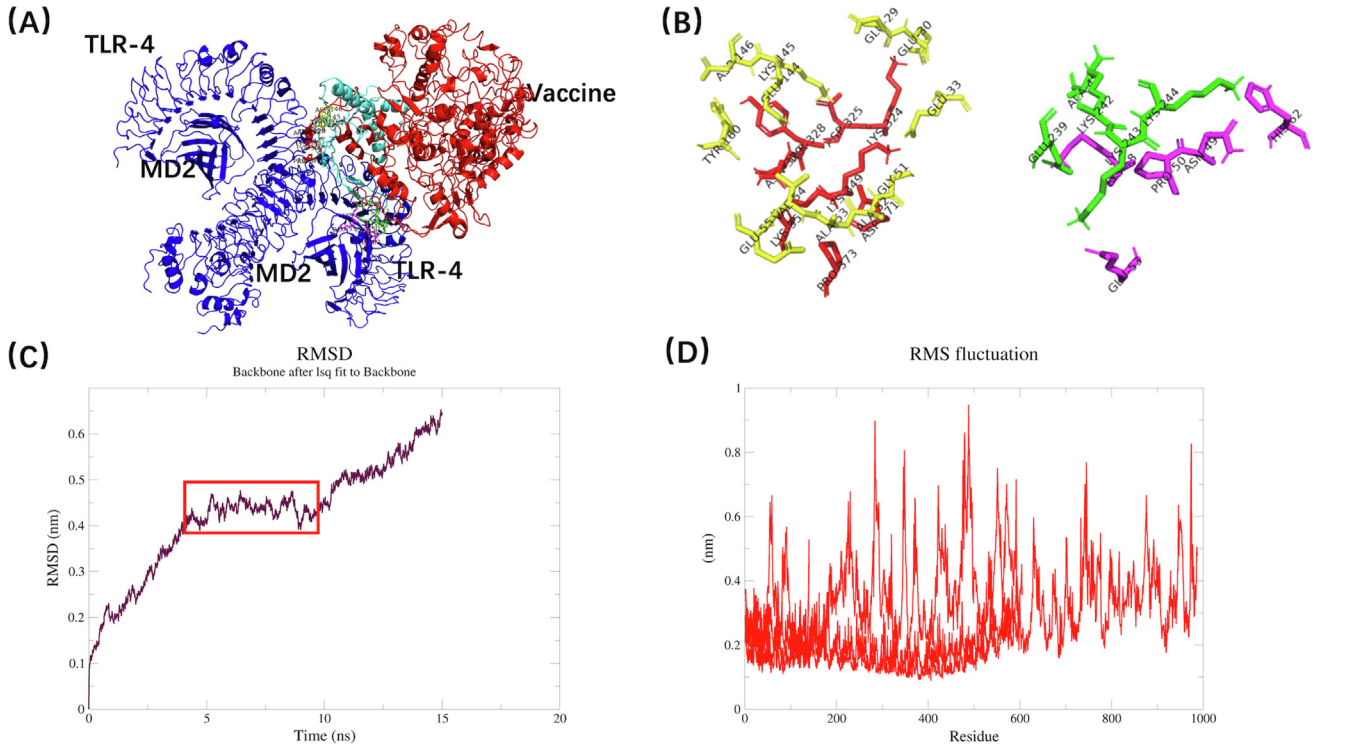

Fig. 4. Stable complexes of the vaccine protein docking with human TLR-4/MD2 receptor molecules. (A) Schematic representation of the docking results; (B) Interactions with amino acid residues; (C) RMSD plot obtained for the vaccine protein backbone after making complex with the TLR4/MD2 as receptor, the red mark RMSD plot reveals that it reaches up to equilibrium within 5–10 ns with the RMSD value of 0.45 nm; (D) RMSF result showing the fluctuation of side chain residue of vaccine protein in complex form with TLR4/MD2. (For interpretation of the references to color in this figure legend, the reader is referred to the web version of this article.)

eight amino acid residues of TLR-4 B chains and the MD2 chain (D) of the five amino acid residues (Fig. 4B), of which ten amino acid residues in the vaccines were able to produce 11 hydrogen bonds with nine amino acid residues of the receptors, and the remaining seven amino acid residues provided hydrophobic interactions. Nine amino acid residues in the adjuvant region were found to be involved in the interaction: Glu 30 (A), Glu 29 (A), Glu 33 (A), Glu 55 (A), Val 54 (A), Ala 53 (A), Ala 52 (A), Ala 45 (A). Additionally, four of these formed the hydrogen bond interaction: Glu 29 (A) - Lys 324 (B); Glu 33 (A) - Lys 349 (B); Ala 53 (A) - Lys 351 (B); Ala 52 (A) - Lys 351 (B). The RMSD plot obtained for the backbone atom of docked complex reveals that it reaches up to equilibrium within 5–10 ns with the RMSD value of 0.45 nM (Fig. 4C). RMSF plot for the side chain of docked complex reveals that the complex is stable with the value of 0.4 nM (Fig. 4D), and the binding free energy is −114.1217 kcal/mole. All these results are showing complex stability.

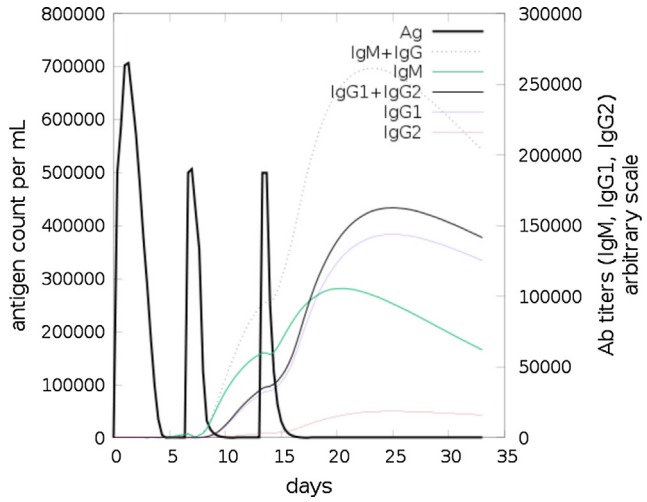

Fig. 5. Antigen and immunoglobulins. Antibodies are sub-divided per isotype.

3.8. Optimization gene codon and expression of designed vaccine

In order to improve the stability and efficiency of expression of the designed multivalent enterovirus vaccines in the prokaryotic expression system, we carried out in silico cloning. The vaccine DNA sequence based on *E. coli* expression host codon optimization was obtained. The final clone expression plasmid size was 8330 pairs of base pairs (Supplementary Fig. 3A and Supplementary data 1). The acquisition of A5V was obtained by constructing a BL21-expressing strain and inducing the expression of purified soluble proteins (Supplementary Fig. 3B).

3.9. A5V immunogenicity evaluated in silico and in vivo

With the strengthening of immunity, the level of immunoglobulin (IgG, IgM) gradually increased (Fig. 5). Although the level of antibody decreased along with the clearance of the antigen, Memory B cells and memory TH cells remained at a high level after antigen clearance (Supplementary Fig. 4A, C). These results indicate

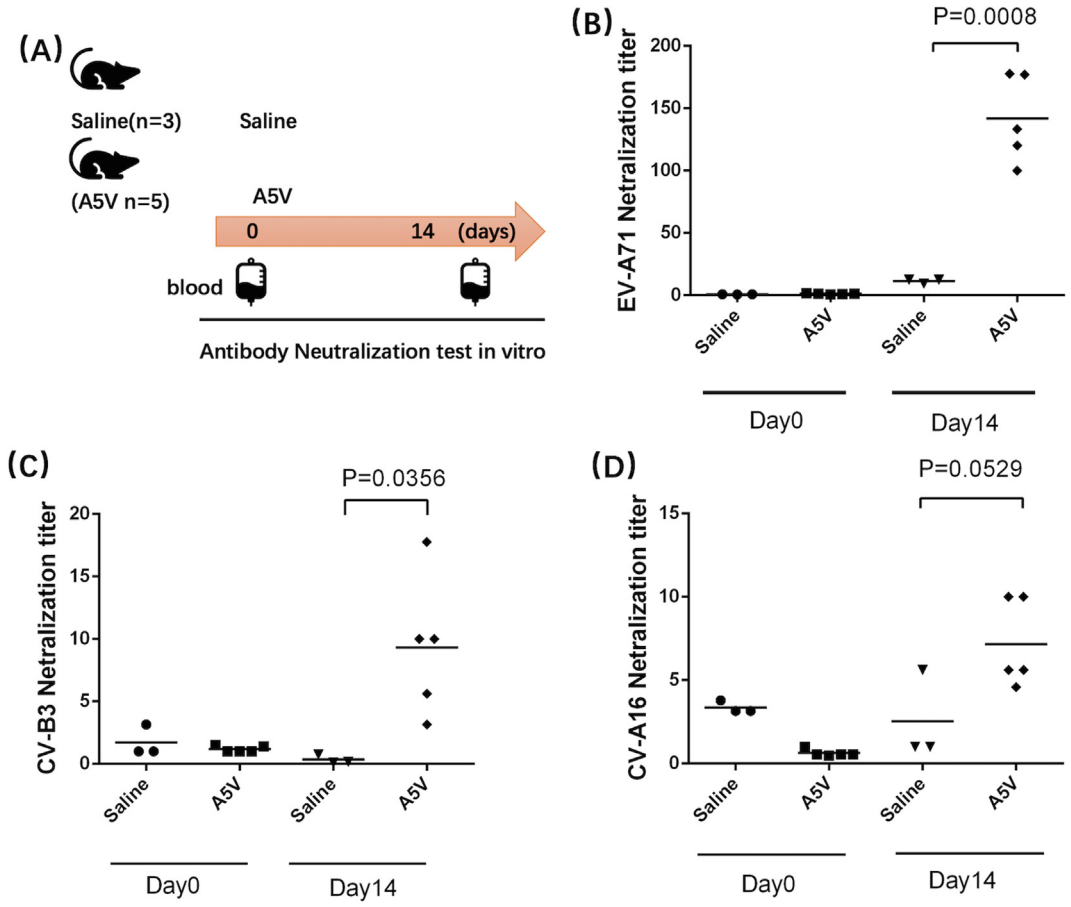

Fig. 6. A5V immunogenicity evaluated in vivo. (A) schematic representation of the mice immunization and neutralization test; (B–D) antisera neutralized EV-A71, CV-B3, CV-A16 in vitro, Statistical significance was determined by the Student's two-tailed *t*-test.

development of immune memory and consequently increased clearance of the antigen upon subsequent exposures. Activation of large numbers of TCL cells and high levels of IFN-γ (Supplementary Fig. 4B, D) suggested that the protein vaccine could activate the cellular immune response. The vaccine with the 50 s ribosomal protein L7/L12 adjuvant elicited a slightly stronger immune response than the vaccine without the adjuvant (Supplementary Fig. 5), further supporting the intrinsic antigenicity properties mentioned earlier. In animal experiments, the schematic is shown in Fig. 6A, In vitro neutralization experiments of mice on day 14 of immunization showed significant neutralization of EV-A71 and CV-B3 virus strains by immune sera, with a highly significant effect of P value 0.0008 for EV-A71 strains (Fig. 6B) and a significant effect of P value 0.0356 for CV-B3 strain neutralization (Fig. 6C). From the results of the analysis, it can be seen that the immune serum also neutralized the CV-A16 strain, although the significance P value 0.0529 (Fig. 6D). From the results of in vitro neutralization experiments in which three different enteroviruses were immunized only once, it can be estimated that A5V has ability induced neutralizing antibodies against EV-A71, CV-B3 and CV-A16, indicating that the multivalent enterovirus vaccine can protect against the infection of different enteroviruses.

4. Discussion and conclusion

The outbreak of enteroviruses has resulted in public health problems, worldwide, especially in the Asia Pacific region. This has resulted in increased concern among health authorities, along with the classification of HFMD as a reportable disease and the introduction of a case-based surveillance system [47]. A multi-epitope synthetic peptide vaccine is an ideal choice for simultaneous immunization of multiple enteroviruses. The high mutation rate of the enterovirus RNA and the recombination between different enterovirus strains lead to numerous and complex enterovirus serotypes, leading to difficulty and complexity of vaccine development and subsequent verification and evaluation of the vaccine against various serotypes of the enterovirus. However, epitope-based vaccines are able to ignore these drawbacks. Immunity against any number of enteroviruses can be conferred by selecting highly conserved primary neutralizing epitopes, rather than just a complete live attenuated or inactivated virus as the vaccine. In our study, the neutralization test indicated that antibodies produced in mice only immunized once that neutralized the three viruses with obvious efficacy. Because we didn't test the neutralizing antibody titers that multivalent vaccine induced to CV-A10 and CV-A6, we could not show clearly efficacy of our multivalent vaccine to total five virus, however, the good immunogenicity of our multivalent vaccine was confirmed by in vitro neutralization assay experiments of the three viruses, which indicate that the multivalent enterovirus vaccine can protect against the infection of different enteroviruses. Ling - Ling and Whitton have developed a multivalent vaccine based on small fragments of a gene recombinant vaccine, containing B-cell, cytotoxic T-lymphocyte, and Th epitopes of *sendai* virus, respiratory syncytial virus, lymphocytic choriomeningitis virus (LCMV), vesicular stomatitis virus, *mycobacterium tuberculosis* and mengovirus by induced the corresponding immune response in vivo [48]. In recent times, computational biology has paved the way for better and more effective design processes of vaccines against infectious pathogens [49]. Immune informatics includes online immune databases, tools, and web servers that can significantly reduce the time and cost involved in traditional immune research. In the age of big data, in silico experiments become more and more accurate. The combination of these tools allows us to perform in silico mimic immunization experiments with specific real-world vaccine and could help to speed up vaccine design or clinically oriented research. A multivalent enterovirus vaccine, which provides protection against major enteroviral strain outbreaks worldwide by effectively inducing cellular and humoral immune responses, is very attractive for the prevention of HFMD. The strategy of the enterovirus vaccine with multivalent epitope based on computer algorithm can save cost and time. Based on an immunoinformatic and in vivo immunogenicity analysis, we selected a candidate vaccine with suitable characteristics.

CRediT authorship contribution statement

Huixiong Deng: Methodology, Validation, Formal analysis, Investigation, Data curation, Writing - original draft, Writing - review & editing, Visualization. **Shun Yu:** Methodology, Formal analysis. **Yingzhu Guo:** Validation. **Liming Gu:** Data curation. **Gefei Wang:** Conceptualization, Validation, Formal analysis, Resources, Supervision, Project administration, Funding acquisition, Writing - review & editing. **Zhihui Ren:** Data curation. **Yanlei Li:** Data curation. **Kangsheng Li:** Resources, Supervision. **Rui Li:** Conceptualization, Formal analysis, Resources, Supervision, Project administration, Funding acquisition, Writing - review & editing.

Declaration of Competing Interest

The authors declare that they have no known competing financial interests or personal relationships that could have appeared to influence the work reported in this paper.

Acknowledgements

This work was supported by the grants from National Natural Science Foundation of China (31300761 and 31170852), Natural Science Foundation of Guangdong Province (2018A030313548), Department of Education of Guangdong Province (2020KZDZX1083), and Shantou Science and Technology Bureau.

Appendix A. Supplementary data

Supplementary data to this article can be found online at https://doi.org/10.1016/j.vaccine.2020.03.023.

References

[1] Baggen J, Thibaut HJ, Strating JRPM, Van Kuppeveld FJM. The life cycle of non-polio enteroviruses and how to target it. Nat Rev Microbiol 2018;16:368–81. https://doi.org/10.1038/s41579-018-0005-4.
[2] Fang C-Y, Liu C-C. Recent development of enterovirus A vaccine candidates for the prevention of hand, foot, and mouth disease. Expert Rev Vacc 2018;17:819–31. https://doi.org/10.1080/14760584.2018.1510326.
[3] Lugo D, Krogstad P, Pharmacology M. Enteroviruses in the early 21st century: new manifestations and challenges. Curr Opin Pediatr 2016;28:107–13. https://doi.org/10.1097/MOP.0000000000000303.
[4] Fu X, Mao L, Wan Z, Xu R, Ma Y, Shen L, et al. High proportion of coxsackievirus B3 genotype A in hand, foot and mouth disease in Zhenjiang, China, 2011–2016. Int J Infect Dis 2019;87:1–7. https://doi.org/10.1016/j.ijid.2019.07.012.
[5] Puenpa J, Wanlapakorn N, Vongpunsawad S, Poovorawan Y. The history of enterovirus A71 outbreaks and molecular epidemiology in the Asia-Pacific region. J Biomed Sci 2019;26:75. https://doi.org/10.1186/s12929-019-0573-2.
[6] Klein M, Chong P. Is a multivalent hand, foot, and mouth disease vaccine feasible? Hum Vacc Immunother 2015;11:2688–704. https://doi.org/10.1080/21645515.2015.1049780.
[7] Liu CC, Chow YH, Chong P, Klein M. Prospect and challenges for the development of multivalent vaccines against hand, foot and mouth diseases. Vaccine 2014;32:6177–82. https://doi.org/10.1016/j.vaccine.2014.08.064.
[8] Aswathyraj S, Arunkumar G, Alidjinou EK, Hober D. Hand, foot and mouth disease (HFMD): emerging epidemiology and the need for a vaccine strategy. Med Microbiol Immunol 2016;205:397–407. https://doi.org/10.1007/s00430-016-0465-y.
[9] Zhang Z, Dong Z, Li J, Carr MJ, Zhuang D, Wang J, et al. Protective efficacies of formaldehyde-inactivated whole-virus vaccine and antivirals in a murine

model of coxsackievirus A10 infection. J Virol 2017;91. https://doi.org/10.1128/JVI.00333-17.
[10] Li R, Liu L, Mo Z, Wang X, Xia J, Liang Z, et al. An inactivated enterovirus 71 vaccine in healthy children. N Engl J Med 2014;370:829–37. https://doi.org/10.1056/NEJMoa1303224.
[11] Zhu FC, Meng FY, Li JX, Li XL, Mao QY, Tao H, et al. Efficacy, safety, and immunology of an inactivated alum-adjuvant enterovirus 71 vaccine in children in China: A multicentre, randomised, double-blind, placebo-controlled, phase 3 trial. Lancet 2013;381:2024–32. https://doi.org/10.1016/S0140-6736(13)61049-1.
[12] Mao Q, Cheng T, Zhu F, Li J, Wang Y, Li Y, et al. The cross-neutralizing activity of enterovirus 71 subgenotype C4 vaccines in healthy chinese infants and children. PLoS ONE 2013;8:e79599. https://doi.org/10.1371/journal.pone.0079599.
[13] Zhu F, Xu W, Xia J, Liang Z, Liu Y, Zhang X, et al. Efficacy, safety, and immunogenicity of an enterovirus 71 vaccine in China. N Engl J Med 2014;370:818–28. https://doi.org/10.1056/NEJMoa1304923.
[14] Chong P, Guo MS, Lin FHY, Hsiao KN, Weng SY, Chou AH, et al. Immunological and biochemical characterization of coxsackie virus A16 viral particles. PLoS ONE 2012;7:e49973. https://doi.org/10.1371/journal.pone.0049973.
[15] Saha S, Raghava GPS. Prediction of continuous B-cell epitopes in an antigen using recurrent neural network. Proteins 2006;65:40–8. https://doi.org/10.1002/prot.21078.
[16] Sette A, Peters B, Wang P, Sidney J, Dow C, Mothe B. A Systematic assessment of MHC class II peptide binding predictions and evaluation of a consensus approach. PLoS Comput Biol 2008;4:e1000048. https://doi.org/10.1371/journal.pcbi.1000048.
[17] Reche PA, Hong JG, Reinherz EL. Enhancement to the RANKPEP resource for the prediction of peptide binding to MHC molecules using profiles. Immunogenetics 2004;56:405–19. https://doi.org/10.1007/s00251-004-0709-7.
[18] Greenbaum J. Functional classification of class II human leukocyte antigen (HLA) molecules reveals seven different supertypes and a surprising degree of repertoire sharing across supertypes. Immunogenetics 2011;63:325–35. https://doi.org/10.1007/s00251-011-0513-0.
[19] Dimitrov I, Garnev P, Flower DR, Doytchinova I. EpiTOP-a proteochemometric tool for MHC class II binding prediction. Bioinformatics 2010;26:2066–8. https://doi.org/10.1093/bioinformatics/btq324.
[20] Dhanda SK, Vir P, Raghava GPS. Designing of interferon-gamma inducing MHC class-II binders. Biol Direct 2013;8:30. https://doi.org/10.1186/1745-6150-8-30.
[21] Dhanda SK, Gupta S, Vir P, Raghava GPS. Prediction of IL4 inducing peptides. Clin Dev Immunol 2013;2013:263952. https://doi.org/10.1155/2013/263952.
[22] Weiskopf D, Angelo MA, De Azeredo EL, Sidney J, Greenbaum JA, Fernando AN, et al. Comprehensive analysis of dengue virus-specific responses supports an HLA-linked protective role for CD8 + T cells. Proc Natl Acad Sci USA 2013;110:E2046–53. https://doi.org/10.1073/pnas.1305227110.
[23] Andreatta M, Nielsen M. Sequence analysis Gapped sequence alignment using artificial neural networks : application to the MHC class I system. Bioinformatics 2016;32:511–7. https://doi.org/10.1093/bioinformatics/btv639.
[24] Bhasin M, Raghava GPS. Prediction of CTL epitopes using QM, SVM and ANN techniques. Vaccine 2004;22:3195–204. https://doi.org/10.1016/j.vaccine.2004.02.005.
[25] Larsen MV, Lundegaard C, Lamberth K, Buus S, Lund O, Nielsen M. Large-scale validation of methods for cytotoxic T-lymphocyte epitope prediction. BMC Bioinf 2007;8:1–12. https://doi.org/10.1186/1471-2105-8-424.
[26] Calis JJA, Maybeno M, Greenbaum JA, Weiskopf D, de Silva AD. Properties of MHC class I presented peptides that enhance immunogenicity. PLoS Comput Biol 2013;9:e1003266. https://doi.org/10.1371/journal.pcbi.1003266.
[27] Gupta S, Kapoor P, Chaudhary K, Gautam A, Kumar R. In silico approach for predicting toxicity of peptides and proteins. PLoS ONE 2013;8:e73957. https://doi.org/10.1371/journal.pone.0073957.
[28] Bui H, Sidney J, Li W, Fusseder N, Sette A. Development of an epitope conservancy analysis tool to facilitate the design of epitope-based diagnostics and vaccines. BMC Bioinf 2007;8:316. https://doi.org/10.1186/1471-2105-8-361.
[29] Peters B, Sette A. Generating quantitative models describing the sequence specificity of biological processes with the stabilized matrix method. BMC Bioinf 2005;6:132. https://doi.org/10.1186/1471-2105-6-132.
[30] Negahdaripour M, Nezafat N, Eslami M, Ghoshoon MB, Shoolian E, Najafipour S, et al. Structural vaccinology considerations for in silico designing of a multi-epitope vaccine. Infect Genet Evol 2018;58:96–109. https://doi.org/10.1016/j.meegid.2017.12.008.
[31] Lee SJ, Shin SJ, Lee MH, Lee MG, Kang TH, Park WS, et al. A potential protein adjuvant derived from Mycobacterium tuberculosis Rv0652 enhances dendritic cells-based tumor immunotherapy. PLoS ONE 2014;9:e104351. https://doi.org/10.1371/journal.pone.0104351.
[32] Doytchinova IA, Flower DR. VaxiJen: A server for prediction of protective antigens, tumour antigens and subunit vaccines. BMC Bioinf 2007;8:1–7. https://doi.org/10.1186/1471-2105-8-4.
[33] Cheng J, Randall AZ, Sweredoski MJ, Baldi P. SCRATCH: A protein structure and structural feature prediction server. Nucleic Acids Res 2005;33:72–6. https://doi.org/10.1093/nar/gki396.
[34] Dimitrov I, Bangov I, Flower DR, Doytchinova I. AllerTOP vol 2-A server for in silico prediction of allergens. J Mol Model 2014;20:S4. https://doi.org/10.1007/s00894-014-2278-5.
[35] Magnan CN, Randall A, Baldi P. SOLpro: Accurate sequence-based prediction of protein solubility. Bioinformatics 2009;25:2200–7. https://doi.org/10.1093/bioinformatics/btp386.
[36] Wilkins MR, Gasteiger E, Bairoch A, Sanchez JC, Williams KL, Appel RD, et al. Protein identification and analysis tools in the ExPASy server. Meth Mol Biol 1999;112:531–52. https://doi.org/10.1385/1-59259-584-7:531.
[37] Buchan DWA, Minneci F, Nugent TCO, Bryson K, Jones DT. Scalable web services for the PSIPRED Protein Analysis Workbench. Nucl Acids Res 2013;41:349–57. https://doi.org/10.1093/nar/gkt381.
[38] Roy A, Xu D, Poisson J, Zhang Y. A protocol for computer-based protein structure and function prediction. J Vis Exp 2011:e3259. https://doi.org/10.3791/3259.
[39] Craig DB, Dombkowski AA. Disulfide by Design 2.0: A web-based tool for disulfide engineering in proteins. BMC Bioinf 2013;14:346. https://doi.org/10.1186/1471-2105-14-346.
[40] Heo L, Park H, Seok C. GalaxyRefine: Protein structure refinement driven by side-chain repacking. Nucl Acids Res 2013;41:384–8. https://doi.org/10.1093/nar/gkt458.
[41] Wiederstein M, Sippl MJ. ProSA-web: Interactive web service for the recognition of errors in three-dimensional structures of proteins. Nucl Acids Res 2007;35:407–10. https://doi.org/10.1093/nar/gkm290.
[42] Lovell SC, Davis IW, Arendall WB, De Bakker PIW, Word JM, Prisant MG, et al. Structure validation by Cα geometry: φ, ψ and Cβ deviation. Proteins Struct Funct Genet 2003;50:437–50. https://doi.org/10.1002/prot.10286.
[43] Kringelum JV, Lundegaard C, Lund O, Nielsen M. Reliable B cell epitope predictions: impacts of method development and improved benchmarking. PLoS Comput Biol 2012;8:e1002829. https://doi.org/10.1371/journal.pcbi.1002829.
[44] Vajda Sandor. New additions to the ClusPro server motivated by CAPR. Proteins 2017;85:435–44. https://doi.org/10.1002/prot.25219.
[45] Ra L, Mb S. LigPlot+: multiple ligand-protein interaction diagrams for drug discovery. J Chem Inf Model 2011;51:2778–86. https://doi.org/10.1021/ci200227u.
[46] Rapin N, Lund O, Bernaschi M, Castiglione F. Computational immunology meets bioinformatics: The use of prediction tools for molecular binding in the simulation of the immune system. PLoS ONE 2010;5. https://doi.org/10.1371/journal.pone.0009862.
[47] World Health Organization. A Guide to Clinical Management and Public Health Response for Hand, Foot and Mouth Disease (HFMD). World Heal. Organ. 2011;18. , https://iris.wpro.who.int/bitstream/handle/10665.1/5521/9789290615255_eng.pdf.
[48] An LL, Whitton JL. A multivalent minigene vaccine, containing B-cell, cytotoxic T-lymphocyte, and Th epitopes from several microbes, induces appropriate responses in vivo and confers protection against more than one pathogen. J Virol 1997;71:2292–302.
[49] Azoitei ML, Correia BE, Ban Y-EA, Carrico C, Kalyuzhniy O, Chen L, et al. Computation-guided backbone grafting of a discontinuous motif onto a protein scaffold. Science 2011;334:373–6. https://doi.org/10.1126/science.1209368.